Analog to the pion decay constant in the multiflavor Schwinger model

Jaime Fabián Nieto Castellanos,[1] Ivan Hip,[2] and Wolfgang Bietenholz[1]
[1]*Instituto de Ciencias Nucleares, Universidad Nacional Autónoma de México, A.P. 70-543, C.P. 04510 Ciudad de México, Mexico*
[2]*University of Zagreb Faculty of Geotechnical Engineering, Hallerova aleja 7, 42000 Varaždin, Croatia*

(Received 8 May 2023; accepted 10 October 2023; published 8 November 2023)

We study the Schwinger model with $N_f \geq 2$ degenerate fermion flavors, by means of lattice simulations. We use dynamical Wilson fermions for $N_f = 2$, and reweighted quenched configurations for overlap-hypercube fermions with $N_f \leq 6$. In this framework, we explore an analogue of the QCD pion decay constant F_π, which is dimensionless in $d = 2$, and which has hardly been considered in the literature. We determine F_π by three independent methods, with numerical and analytical ingredients. First, we consider the 2-dimensional version of the Gell-Mann–Oakes–Renner relation, where we insert both theoretical and numerical values for the quantities involved. Next we refer to the δ-regime, i.e., a small spatial volume, where we assume formulas from chiral perturbation theory to apply even in the absence of Nambu-Goldstone bosons. We further postulate an effective relation between N_f and the number of relevant, light bosons, which we denote as "pions". Thus F_π is obtained from the residual "pion" mass in the chiral limit, which is a finite-size effect. Finally, we address the 2-dimensional Witten–Veneziano formula: it yields a value for F_η, which we identify with F_π, as in large-N_c QCD. All three approaches consistently lead to $F_\pi \simeq 1/\sqrt{2\pi}$ at fermion mass $m = 0$, which implies that this quantity is meaningful.

DOI: 10.1103/PhysRevD.108.094503

I. INTRODUCTION

The Schwinger model represents quantum electrodynamics in two space-time dimensions [1]. This model shares several fundamental features with 4-dimensional quantum chromodynamics (QCD), in particular, confinement [2] as well as the division of the gauge configurations into topological sectors.

This model has been solved exactly in the massless case, but not at finite fermion mass, $m > 0$. In that case, analytic approaches are usually based on bosonization and involve some assumptions and approximations.

Here, we consider the Schwinger model with $N_f \geq 2$ degenerate fermion flavors, in Euclidean space-time.

Chiral perturbation theory is a systematic low-energy effective theory of QCD, in terms of light meson fields. Its Lagrangian includes a string of terms, which are Lorentz invariant and chirally symmetric (if we refer to the chiral limit, where the mesons are massless Nambu-Goldstone bosons). The number of these terms is infinite, but they can be hierarchically ordered in powers of the momenta, and truncated. Each term has a coefficient, known as a low-energy constant, which is a free parameter within chiral perturbation theory. It can only be determined from QCD as the underlying, fundamental theory, or from experiment.

To leading order, there is only one term,

$$\mathcal{L} = \frac{F_\pi^2}{4} \partial^\mu \vec{\pi}(x) \cdot \partial_\mu \vec{\pi}(x), \tag{1.1}$$

where $\vec{\pi}$ is the pion field, and the corresponding low-energy constant F_π is known as the *pion decay constant*. It appears in a variety of relations, which are not necessarily related to the pion decay.

Some of these relations occur in an analogous form in the multiflavor Schwinger model. Based on such analogies, we discuss three independent formulations of F_π in the Schwinger model. It is dimensionless in $d = 2$, and the results obtained with these three approaches are all compatible with the value

$$F_\pi \simeq 1/\sqrt{2\pi} \simeq 0.3989, \tag{1.2}$$

in the chiral limit.

In addition, this result is in good agreement with the only previous determination that we are aware of: a study for $N_f = 2$ by Harada *et al.* at strong coupling in a light-cone formulation [3], which considered the relation

$$\langle 0|\partial^\mu J^5_\mu(0)|\pi(p)\rangle = M_\pi^2 F_\pi, \tag{1.3}$$

where J^5_μ is the axial current, and M_π is the "pion" mass. In this manner, Ref. [3] obtained a mild dependence on the (degenerate) fermion mass m,

$$F_\pi(m) = 0.394518(14) + 0.040(1)m/g, \tag{1.4}$$

where g is the gauge coupling, and $F_\pi(0)$ is close to our value in Eq. (1.2).

On the other hand, if one refers directly to the axial current, instead of its divergence,

$$\langle 0|J^5_\mu(0)|\pi(p)\rangle = \mathrm{i}p_\mu F_\pi, \tag{1.5}$$

one seems to arrive at $F_\pi = 0$, so the outcome does depend on the QCD relation to which one establishes an analogy.

The QCD-inspired relations that we refer to are the Gell-Mann–Oakes–Renner relation (Sec. II), the residual pion mass in the δ-regime (Sec. III), and the Witten-Veneziano formula (Sec. IV). Finally, we present our conclusions and an appendix about finite-size effects on M_π. Preliminary results of this work are presented in a thesis [4] and two proceeding contributions [5].

II. 2d GELL-MANN–OAKES–RENNER RELATION

Back in 1992, Smilga derived the relation [6],

$$m\Sigma = CM_\pi^2, \tag{2.1}$$

where Σ is the chiral condensate, which—in terms of the fermion fields—takes the usual form $\Sigma = -\langle\bar{\Psi}\Psi\rangle$. In the effective Lagrangian for QCD at small but nonzero quark masses, F_π and Σ are the two leading low-energy constants.

However, Smilga did not specify the constant C. That was accomplished in Refs. [7–9]: the bosonized 2-flavor Schwinger model leads to a Schrödinger-type equation, and in this framework, these works studied the interactions of (quasi)zero modes due to the chiral anomaly and the fermion masses. This led to an interesting formula [Eq. (37) in Ref. [7]], which—in our notation and at zero vacuum angle—reads

$$\Sigma = \frac{M_\pi^2}{4\pi m}. \tag{2.2}$$

This relation is explained in detail in Ref. [9]. In addition, Ref. [7] also derived expressions for M_π in terms of m, g, and the volume, in three different regimes. By inserting M_π into Eq. (2.2), the authors obtained formulas for Σ in each of these regimes.

However, that work did not relate Eq. (2.2) to the "pion decay constant", which we are interested in. This can be achieved by invoking the Gell-Mann–Oakes–Renner relation [10], which is well-known in QCD,

$$F_\pi^2(m) = \frac{2m}{M_\pi^2}\Sigma. \tag{2.3}$$

If we postulate the same relation in the multiflavor Schwinger model, and combine it with Eq. (2.2), we arrive at

$$F_\pi = \frac{1}{\sqrt{2\pi}}, \tag{2.4}$$

without any mass dependence.

Alternatively—without relying on the approximations in the bosonization approach—we can numerically compute the quantities on the right-hand side of Eq. (2.3) in order to derive results for $F_\pi(m)$. Such results are shown in Fig. 1: they were obtained based on quenched configurations on a lattice of size $V = 24 \times 24$, generated at $\beta = 4$ and $\beta = 6$, and reweighting with the overlap-hypercube fermion determinant, for the cases of $N_\mathrm{f} = 2, \ldots, 6$ degenerate fermion flavors. In Appendix A, we discuss the reliability of reweighting in such cases.

The overlap-hypercube Dirac operator is obtained by using the overlap formula [11], which solves the Ginsparg-Wilson relation [12]. This guarantees an exact, lattice-modified chiral symmetry [13]. However, for the kernel, we do not insert the usual Wilson operator, but a truncated perfect hypercube fermion operator [14]. Compared to the standard overlap formulation, this improves the scaling behavior, approximate rotation invariance, and the level of locality, as demonstrated in quenched QCD [15]. The 2-dimensional version that we use in the Schwinger model was proposed in Ref. [16], and applied also in Refs. [17,18].

Thanks to the chiral symmetry of the overlap-hypercube operator, we can insert the bare fermion mass m, and reliably calculate M_π even at small m. Σ is computed from the spectrum of the Dirac operator,

$$\Sigma(m) = \frac{1}{V}\left\langle \sum_k \frac{1}{\lambda_k + m} \right\rangle, \tag{2.5}$$

where the Dirac eigenvalues λ_k are mapped from the Ginsparg-Wilson circle (with center 1 and radius 1) to the imaginary axis (their location in the continuum limit) by means of a Möbius transform, $\lambda_k \to \lambda_k/(1 - \lambda_k/2)$.

Figure 1 shows that the results for $F_\pi(m)$ are consistently in the magnitude of 0.4. With 30,000 (10,000) configurations at $\beta = 6$ ($\beta = 4$) and for $m \gtrsim 0.2$ (in lattice units), the numerical values are quite precise. This figure refers to the third regime in the case distinction of Eq. (36) in Ref. [7], which is characterized (among other conditions) by $L_t M_\pi \gg 1$ (in a volume $L \times L_t$). We also observe consistent agreement in the ranges $\beta = 4, \ldots, 6$ and $N_\mathrm{f} = 2, \ldots, 6$, which indicates that—in this range—the value of $F_\pi(m)$ hardly depends on the gauge coupling and on the number of flavors.

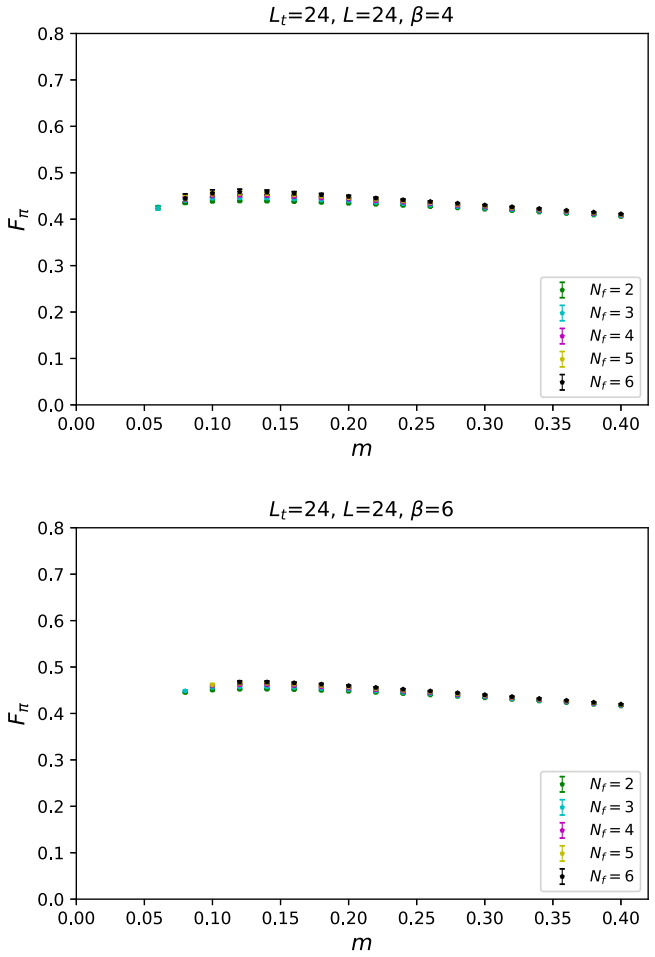

FIG. 1. Values for F_π obtained from the Gell-Mann–Oakes–Renner relation (2.3) for $N_\mathrm{f} = 2, \ldots, 6$ flavors, at fermion masses $0.05 \le m \le 0.4$. The data are obtained from quenched simulations at $\beta = 4$ (above) and at $\beta = 6$ (below) with overlap-hypercube reweighting, which works well, but for fermion mass $m \lesssim 0.05$, the results are affected by finite-size effects on M_π. We see convincing agreement for different N_f, and hardly any difference for the different gauge couplings; hence, the continuum limit seems smooth. In all cases, the extrapolations to the chiral limit are compatible with $F_\pi \simeq 0.4$.

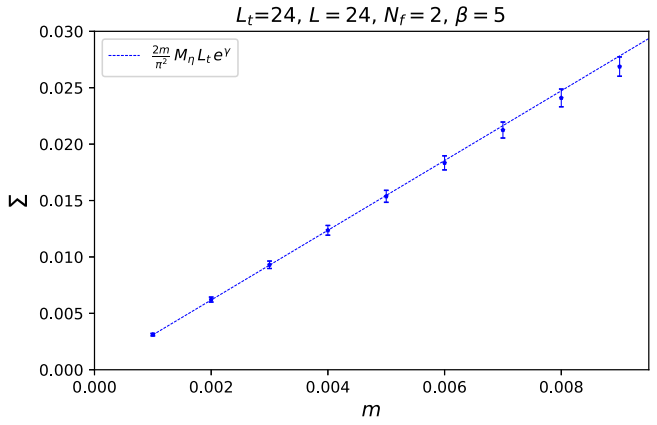

FIG. 2. The chiral condensate, measured for $N_\mathrm{f} = 2$, at $\beta = 5$ on a 24×24 lattice, based on the Dirac spectrum according to Eq. (2.5). It is compared to an asymptotic formula for small m given in Ref. [7], where M_η represents the "η-meson" mass in the chiral limit, see Eq. (4.4). We see that reweighting works very well even for fermion masses down to $m = 0.001$ (cf. Appendix A), but the Gell-Mann–Oakes–Renner relation for F_π, Eq. (2.3), also involves M_π, which is amplified by finite-size effects.

At smaller fermion mass, we enter the second regime of Eq. (36) in Ref. [7], where $L_t M_\pi \ll 1$ (the spatial size L remains large, so there is no relevant residual pion mass due to finite size effects). Here, the errors increase visibly, and if m is too small, even the measured values are not reliable anymore: we still obtain good results for Σ, as we see in Fig. 2, which shows a comparison with predictions in Ref. [7]. This also implies that reweighting works well, at least for $N_\mathrm{f} = 2$ flavors, even down to tiny fermion masses, in agreement with earlier results in Ref. [19].[1] However, at tiny values of m, the pion mass M_π suffers from significant finite-size effects, since the product LM_π is not large anymore. Moreover, in that regime, there is a discrepancy between different ways to measure M_π, as we point out in Appendix B.

For all N_f that we included, we observe in Fig. 1 a slight maximum of $F_\pi(m)$ between $m = 0.1$ and 0.15. At even smaller fermion mass m, $F_\pi(m)$ decreases, and the chiral extrapolation is again compatible with $F_\pi(0) = 1/\sqrt{2\pi}$, although at tiny m the finite-size effects on M_π and the large statistical errors prevent a precise chiral extrapolation.

On the other hand, in some circumstances, the increase of M_π due to finite-size effects can also be used to extract physical information. This is addressed in the next section.

III. F_π FROM THE RESIDUAL PION MASS IN THE δ-REGIME

The approach of this section refers to chiral perturbation theory, which is a systematic effective field theory for low-energy QCD, cf. Sec. I. One writes a general Lagrangian—with all terms allowed by the symmetries—in terms of pseudo-Nambu-Goldstone boson fields. In 2-flavor QCD, the fields represent the pions, which pick up a small mass M_π through nonzero masses of the u- and d-quark, and by finite-size effects (if the volume is finite).

The latter are negligible in the most commonly used setting, the p-regime of chiral perturbation theory: here the space-time volume is large, in all directions, compared to the correlation length $1/M_\pi$. From a theoretical perspective, it is also instructive to study the ϵ-regime of a small space-time volume, and the δ-regime, with a small spatial box L^3 but a large extent L_t in (Euclidean) time,

[1]The reliability of reweighting, depending on N_f and m, is further discussed in Appendix A.

$L_t \gg L = \mathcal{O}(1/M_\pi)$. In the ϵ- and δ-regimes, finite-size effects give rise to a significant energy gap; hence, the pions have a residual mass M_π^{R} even in the chiral limit of massless quarks.

Here, we focus on the *δ-regime:* it represents a quasi-1-dimensional field theory, which formally corresponds to a quantum mechanical system. Leutwyler introduced this regime in Ref. [20]: he employed the picture of a quantum mechanical rotor with the energy gap,

$$M_\pi^{\mathrm{R}} = \frac{N_\pi}{2\Theta}, \tag{3.1}$$

where N_π is the number of pions (or generally, of pseudo-Nambu-Goldstone bosons) involved. The challenge is to compute the "moment of inertia" Θ. Leutwyler also established the appropriate rules for the δ-expansion, and to leading order (LO) he obtained $\Theta = F_\pi^2 L^3$.

This expansion was extended to the next-to-leading order (NLO) by Hasenfratz and Niedermayer, who referred to an O(N) model in $d > 2$ dimensional Euclidean space [21]. According to the Goldstone theorem, the spontaneous symmetry breaking pattern $\mathrm{O}(N) \to \mathrm{O}(N-1)$ yields $N-1$ Nambu-Goldstone bosons, which is the number to be inserted for N_π in Eq. (3.1), along with

$$\Theta = F_\pi^2 L^{d-1}\left[1 + \frac{N_\pi - 1}{2\pi F_\pi^2 L^{d-2}}\left(\frac{d-1}{d-2} - \frac{1}{2}\alpha_{1/2}^{(d-1)}(1)\right)\right], \tag{3.2}$$

where F_π has the mass dimension $d/2-1$. [The constant $\alpha_{1/2}^{(d-1)}(1)$ is a shape coefficient; its numerical values are given for symmetric boxes in various dimensions in Ref. [22].] Since that work refers to $d > 2$, Nambu-Goldstone bosons are present, and there was no problem with the pole at $d = 2$.

Later, the NNLO was investigated in Refs. [23,24]. At this order, the subleading low-energy constants $l_1, \ldots, l_4$ enter. Comparison of simulation data with the formulas of Ref. [23] yielded, in particular, a sensible value for the controversial coupling l_3 [25]. Another numerical study explored the transitions from the δ-regime to the ϵ- and p-regimes [26].

The current study refers to $d = 2$, with a volume $L_t \times L$, $L_t \gg L$. Here, the Mermin-Wagner-Coleman theorem excludes Nambu-Goldstone bosons in the strict sense, but it is known that the "pions" at small but finite fermion mass behave similarly to pseudo-Nambu-Goldstone bosons in higher dimensions. (At $m = 0$ they decouple, thus avoiding a contradiction with the Mermin-Wagner-Coleman theorem [27].) For considerations about the applicability of chiral perturbation theory in the Schwinger model, we refer to Ref. [28].

Due to the singularity at the NLO, we can only refer to the LO, so we start from the hypothesis,

$$M_\pi^{\mathrm{R}} = \frac{N_\pi}{2F_\pi^2 L}. \tag{3.3}$$

The basic prediction reduces to $M_\pi^{\mathrm{R}} \propto 1/L$, which is plausible on dimensional grounds. If this is observed numerically, we have another way to determine F_π, up to the question how N_π should be interpreted in this setting, with N_{f} massless fermion flavors.

Part of the literature, for instance, Refs. [29,30], assumes $N_{\mathrm{f}}^2 - 1$ "pions". This matches the number of Nambu-Goldstone bosons in the spontaneous symmetry breaking $\mathrm{SU}(N_{\mathrm{f}}) \otimes \mathrm{SU}(N_{\mathrm{f}}) \to \mathrm{SU}(N_{\mathrm{f}})$ in $d \geq 3$ dimensions according to the Goldstone theorem. On the other hand, the literature which analyzes the multiflavor Schwinger model with bosonization usually deals with $N_{\mathrm{f}} - 1$ "pions" [7–9,31,32].

In fact, in the case $N_{\mathrm{f}} = 2$, we obtain values for F_π, which are consistent with the results based on the Gell-Mann–Oakes–Renner relation, if and only if we insert $N_\pi = 1$.

When we proceed to $N_{\mathrm{f}} > 2$, however, we see that the bosonization formula $N_{\mathrm{f}} - 1$ does not work anymore. So we take a pragmatic point of view and adjust the number of "pionic" degrees of freedom, which are manifest in formula (3.3). We obtain consistent values for F_π, to an impressively high accuracy, if we insert the effective formula,

$$N_\pi = \frac{2(N_{\mathrm{f}} - 1)}{N_{\mathrm{f}}}, \tag{3.4}$$

although—according to this formula—N_π is a noninteger for $N_{\mathrm{f}} \geq 3$.

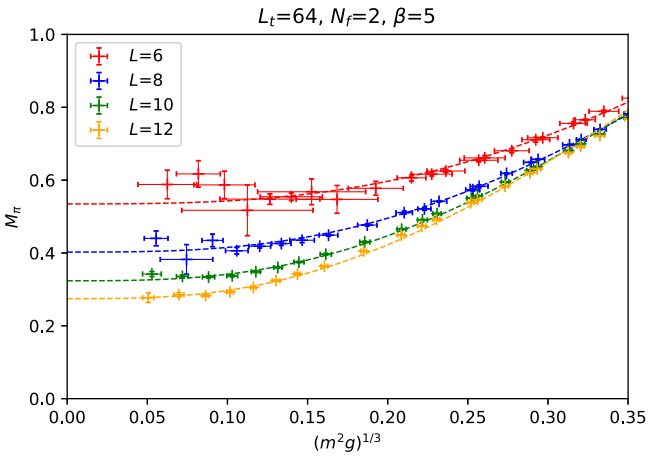

FIG. 3. Simulation results for the "pion" mass M_π in the δ-regime, $L \ll L_t$ (with $L_t = 64$), using dynamical Wilson fermions. For a small fermion mass m (determined by the PCAC relation) and a small spatial extent L, significant errors occur, as expected for Wilson fermions. Still, the full range of fermion masses enables sensible extrapolations to the residual "pion" mass M_π^{R} in the chiral limit $m \to 0$.

Let us substantiate this statement by presenting our simulation results. We first refer to $N_f = 2$ flavors of dynamical Wilson fermions, which are convenient to simulate. We set the Wilson parameter to 1 and used the hybrid Monte Carlo (HMC) algorithm [33], following the scheme, which was established in Ref. [34] for the 2-flavor Schwinger model: trajectories consist of 10 steps, with the step size being dynamically adjusted for a Metropolis acceptance rate close to 0.8. We monitored the autocorrelations of several observables—including the topological charge—and separated the measurements by twice the maximal autocorrelation time, in order to obtain practically decorrelated data sets. In this way, we generated 10,000 configurations for each parameter set.

Of course, the results for Wilson fermions are plagued by additive mass renormalization. As usual for nonchiral lattice fermions, the renormalized fermion mass m is measured based on the PCAC relation. Figure 3 shows results for the "pion" mass M_π in the δ-regime, with $L_t = 64 \gg L$ ($L = 6$, 8, 10, 12), which is plotted against the dimensionless parameter $(m^2 g)^{1/3}$, at $\beta = 1/g^2 = 5$ (still in lattice units). As a generic property, at decreasing, small values of m and $(m^2 g)^{1/3}$, the statistical errors of M_π and, in particular, of m itself increase rapidly (at fixed statistics), but the complete set of results allows for smooth fits with sensible extrapolations to the chiral limit $m = 0$.

Figure 4 shows these extrapolated values of $M_\pi(m = 0)$ as a function of the spatial size L over the range of $L = 6, \ldots, 12$. A fit confirms the expected behavior $M_\pi(m = 0) \propto 1/L$ to high accuracy, in particular, up to $L = 11$. The proportionality constant is a fitting parameter, which—inserted in Eq. (3.3)—yields an F_π value close to the one in Eq. (1.2), $F_\pi = 0.3923(6)$.

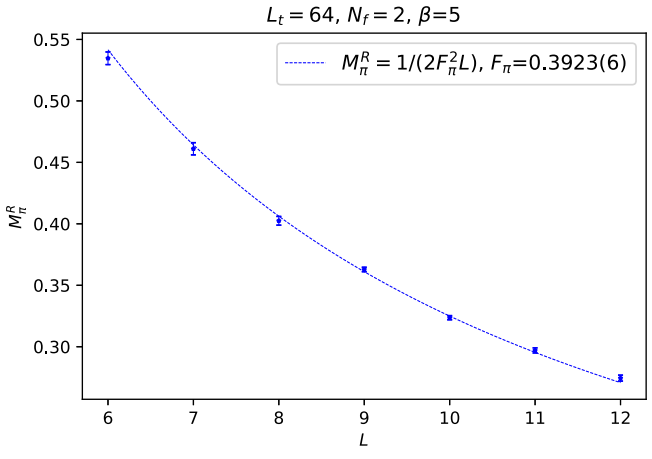

FIG. 4. The residual "pion" masses M_π^R in the δ-regime, obtained from simulations of two flavors of dynamical Wilson fermions and extrapolated to the chiral limit according to Fig. 3, in spatial volumes $L = 6, \ldots, 12$. The data follow well a fit proportional to $1/L$, and the coefficient corresponds to $F_\pi = 0.3923(6)$.

TABLE I. Results for F_π, obtained by fits to Eqs. (3.3) and (3.4), with $N_f = 2$, at three values of β.

$\beta = 1/g^2$	3	4	5
F_π	0.3887(7)	0.3877(11)	0.3923(6)

We obtained very similar results at $\beta = 3$ and $\beta = 4$. The corresponding figures are included in the first proceeding contribution cited in Ref. [5]. We do not reproduce these plots here, since they look almost identical to Figs. 3 and 4, but we display the F_π values obtained in this manner at three gauge couplings in Table I (the values are slightly modified due to improved data analysis). They coincide to percent level, thus providing clear evidence that the continuum limit is again very smooth, as we observed before in the consideration of Sec. II.

Next, we proceed to results that we obtained with overlap-hypercube fermions, by using 10,000 gauge configurations that we generated quenched[2] at $\beta = 4$, which were reweighted again for the case of $N_f = 2$ flavors. As we see in Fig. 5, the exact, lattice modified chirality of the overlap-hypercube fermions strongly suppresses the statistical fluctuations at relatively small fermion mass m, which—in this case—is directly taken from the Lagrangian. Thus, in this approach, the values for $M_\pi(m = 0)$ are quite precise. They represent the residual "pion" mass in the δ-regime with $L_t = 32$ and $L = 4, \ldots, 12$. For a further discussion of the reweighting approach, we refer again to Appendix A.

Figure 6 shows that these safely extrapolated values again follow very well a behavior $M_\pi(m = 0) \propto 1/L$, at least for $L < 12$. Here, the fitting constant leads to

$$F_\pi = 0.3988(1), \tag{3.5}$$

in remarkable proximity to the result obtained with Wilson fermions, and in perfect agreement with formula (1.2).

Finally, we extend the study with quenched and overlap-hypercube reweighted configurations up to $N_f = 6$ degenerate flavors, as in Sec. II. Figure 7 illustrates the residual "pion" masses against the spatial lattice size $L = 4, \ldots, 12$. As N_f increases, the behavior $\propto 1/L$ is observed only up to $L = 6$; at somewhat larger L, the residual "pion" mass stays below this proportionality relation.

However, when we restrict the fit to the range where the relation $M_\pi^R \propto 1/L$ is well approximated, we consistently obtain $F_\pi = 0.399(1)$ over this range of N_f, if we insert the effective formula (3.4). This underscores that the value $F_\pi = 1/\sqrt{2\pi}$ is meaningful, and that Eq. (3.4) correctly captures

[2]The quenched configurations used here and in other sections were generated with the same HMC algorithm, by setting the fermion determinant to a constant.

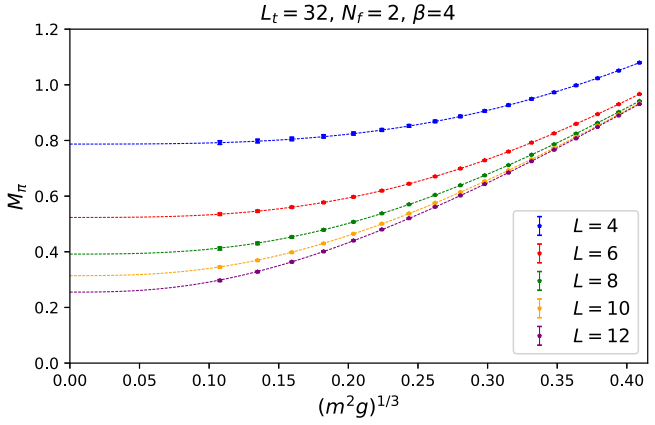

FIG. 5. Like Fig. 3, but here the "pion" mass M_π is measured with overlap-hypercube fermions, using quenched, reweighted gauge configurations, generated at $\beta = 4$. In contrast to Fig. 3, this yields small errors and smooth chiral extrapolations for all spatial sizes $L = 4, \ldots, 12$ under consideration.

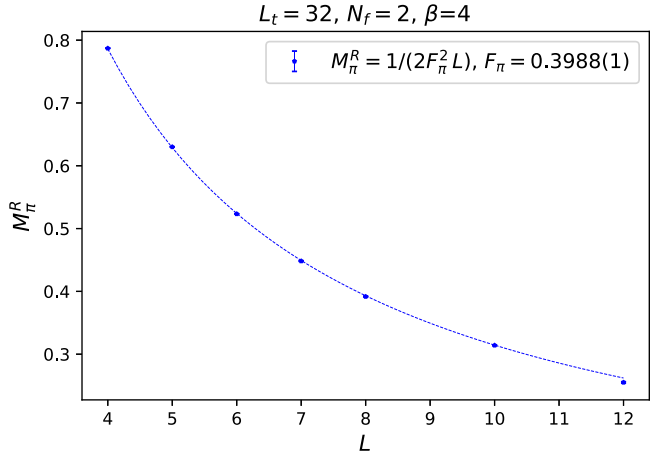

FIG. 6. Like Fig. 4, but now with data obtained from the extrapolation of overlap-hypercube fermions results, see Fig. 5. Again, the fit to the conjectured behavior $M_\pi^{\mathrm{R}} \propto 1/L$ works very well for $L < 12$, and we extract $F_\pi = 0.3988(1)$. This value is well compatible with further results that we obtained for F_π by employing different methods, and in perfect agreement with formula (1.2).

the number of "pionic" degrees of freedom which are manifest in the δ-regime (even if this number is noninteger). We add that any attempts to extend the fits $\propto 1/L$ at large N_{f} up to larger spatial size L lead to an unsatisfactory fitting quality (a modified power of L would be required); hence, they do not provide alternative F_π results.

IV. WITTEN-VENEZIANO FORMULA IN THE SCHWINGER MODEL

The Witten-Veneziano formula is well-known in the framework of QCD [35]: it refers to the 't Hooft large-N_{c} limit, which keeps the product $g_{\mathrm{s}}^2 N_{\mathrm{c}}$ constant (g_{s} is the strong gauge coupling and N_{c} the number of colors). This

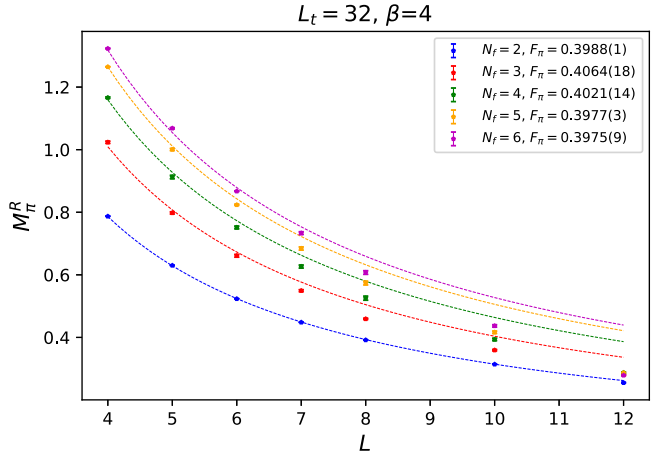

FIG. 7. Residual "pion" masses M_π^{R} in the δ-regime ($L_t = 32$) for a variety of spatial sizes $L \ll L_t$, and $N_{\mathrm{f}} = 2, \ldots, 6$ flavors. We show chiral extrapolations of quenched, reweighted results with overlap-hypercube fermions, at $\beta = 4$. The fits were performed in the range where they are successful, i.e., in the full range for $N_{\mathrm{f}} = 2$ and for $L \leq 6$ for $N_{\mathrm{f}} > 2$. They lead to highly consistent values for F_π, if we apply the effective formula (3.4).

limit overcomes the axial anomaly of chiral 3-flavor QCD. Hence, the spontaneous symmetry breaking pattern takes the form $\mathrm{U(3)_L} \otimes \mathrm{U(3)_R} \to \mathrm{U(3)_{L=R}}$ (where the subscripts L and R denote the quark chiralities), and we obtain a nonet of Nambu-Goldstone bosons: they correspond to the pions, the kaons, and the mesons η and η', which are all massless in this limit.

The Witten-Veneziano formula expresses the mass that the η'-meson picks up due to the leading $1/N_{\mathrm{c}}$ corrections. For the more general case of N_{f} massless quark flavors, this mass is given by

$$M_{\eta'}^2 = \frac{2N_{\mathrm{f}}\chi_{\mathrm{t}}^{\mathrm{q}}}{F_{\eta'}^2}, \tag{4.1}$$

where $\chi_{\mathrm{t}}^{\mathrm{q}}$ is the quenched topological susceptibility, which can be measured by means of lattice simulations. In this particular case, the quenched value is relevant, because quark loops do not contribute to this order in the $1/N_{\mathrm{c}}$ expansion. Moreover, in this order, the pion decay constant coincides with the η'-decay constant,

$$F_\pi = F_{\eta'}. \tag{4.2}$$

Inserting the experimental value of $F_\pi \simeq 92.4$ MeV and simulation results for $\chi_{\mathrm{t}}^{\mathrm{q}}$, see, in particular, Ref. [36], (roughly) confirm the observed mass $M_{\eta'} \simeq 958$ MeV. Thus, the fact that η' is far heavier than the light meson octet (and even a little heavier than a nucleon) is explained as a topological effect. This is the quantitative solution to the U(1) problem.

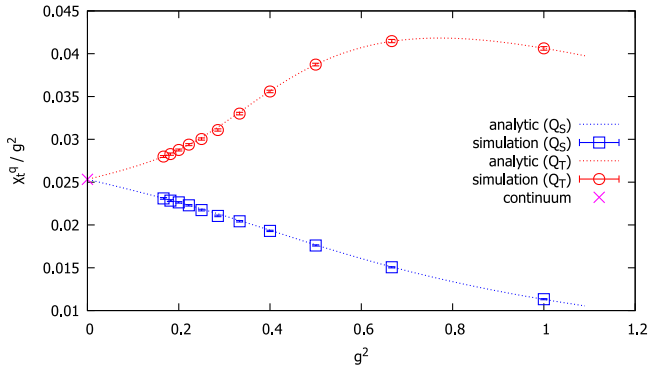

FIG. 8. The quenched topological susceptibility χ_t^q, for two different lattice formulations of the topological charge density [standard plaquette term θ_P and $\sin(\theta_P)$]. In the latter case, the topological charge $Q_S = \sum_P \sin(\theta_P)/2\pi$ can be computed analytically [39], while in case of $Q_T = \sum_P \theta_P/2\pi$ the sum over the plaquettes can be computed numerically [38]. In both cases, the values are in excellent agreement with our simulation results. Both formulations consistently lead to the continuum limit with $\chi_t^q/g^2 = 1/4\pi^2$, which was derived in Ref. [37].

According to Seiler and Stamatescu, the Witten-Veneziano relation is actually on more solid ground in the framework of the Schwinger model with $N_f \geq 2$ massless fermion flavors [37]. In the chiral limit, it takes the form

$$M_\eta^2 = \frac{2N_f}{F_\eta^2}\chi_t^q, \tag{4.3}$$

where the "η-meson" is the meson-type singlet state. Its mass has been computed analytically [31],

$$M_\eta^2 = \frac{1}{\pi}N_f g^2. \tag{4.4}$$

Reference [37] further derived the following relation for the quenched, topological susceptibility (in the continuum and infinite volume),

$$\chi_t^q = \frac{g^2}{4\pi^2}. \tag{4.5}$$

Figure 8 shows results for χ_t^q/g^2 obtained for two lattice formulations of the topological charge,

$$Q_T = \sum_P \theta_P/2\pi, \qquad Q_S = \sum_P \sin(\theta_P)/2\pi. \tag{4.6}$$

The sums run over all plaquettes P, and θ_P is the plaquette discretization of the topological density $\epsilon_{\mu\nu}\partial_\mu A_\nu$. $Q_T \in \mathbb{Z}$ is the standard formulation, which can be numerically evaluated to high precision (see, e.g., Ref. [38]). For the alternative formulation Q_S, the lattice topological charges are, in general, noninteger, but Ref. [39] derived an analytic formula at finite g; i.e., at finite lattice spacing, in terms of Bessel functions, $\beta\chi_t^q = I_1(\beta)/[4\pi^2 I_0(\beta)]$. In both cases, we computed χ_t^q at finite g also with Monte Carlo simulations. The results agree accurately, and the continuum limit smoothly leads to the value given in Eq. (4.5), for both formulations, as Fig. 8 shows. This result is also in agreement with Ref. [19].

Inserting Eqs. (4.4) and (4.5) into Eq. (4.3), we obtain

$$F_\eta = \frac{1}{\sqrt{2\pi}}. \tag{4.7}$$

At this point, we push the analogy to large-N_c QCD further and assume $F_\pi = F_\eta$. We are not aware of a basic justification of this step, but it exactly confirms once more formula (1.2).

V. SUMMARY AND CONCLUSIONS

In this work, we have attracted attention to a dimensionless constant, which plays a relevant role in the multiflavor Schwinger model, but which has been ignored in most of the literature. The only exception is a study by Harada *et al.* [3] in the light-cone formulation, which led to the result that we quoted in Eq. (1.4).

By analogy to specific aspects of QCD, we denote this constant as F_π, as it was done before in Ref. [3]. We derived its value by another three independent methods, which all provide consistent results. In particular, referring to the 2d Gell-Mann–Oakes-Renner relation and inserting formulas from bosonization approaches [6–9] leads to $F_\pi = 1/\sqrt{2\pi}$, which is also compatible with simulation results. The residual "pion" mass in the δ-regime confirms this value to a good precision, if we rely on relations of chiral perturbation theory even in the absence of Nambu-Goldstone bosons, and on our effective formula (3.4) for the number of light degrees of freedom. Finally, the Witten-Veneziano formula yields $F_\eta = 1/\sqrt{2\pi}$, and if we identify $F_\pi = F_\eta$, as in large-N_c QCD, we arrive once more at the same value for F_π.

The first method seems most robust. The latter two involve some *ad hoc* assumptions, which are, however, motivated from analogies to QCD. The impressive agreement of the results for F_π cannot be by accident, so we conclude that these *ad hoc* assumptions are—in this context—sensible. This concerns, in particular, our effective formula (3.4) for the "pionic" degrees of freedom, which are manifest in the δ-regime, as well as the relation $F_\pi = F_\eta$. It further implies that the constant $F_\pi = 1/\sqrt{2\pi}$ is indeed relevant for the multiflavor Schwinger model, in particular for the case $N_f = 2$. The underlying reason, as well as further appearances of F_π in the Schwinger model, remain to be explored.

ACKNOWLEDGMENTS

We thank Stephan Dürr, Christian Hoelbling, and Satoshi Iso for helpful comments. The code was developed

at the cluster Isabella of the Zagreb University Computing Centre (SRCE), and the production runs were performed at the cluster of the Instituto de Ciencias Nucleares, UNAM. This work was supported by the Faculty of Geotechnical Engineering of Zagreb University through the project "Change of the Eigenvalue Distribution at the Temperature Transition" (Grant No. 2186-73-13-19-11), by UNAM-DGAPA through PAPIIT projects IG100219 and IG100322, and by the Consejo Nacional de Humanidades, Ciencia y Tecnología (CONAHCYT).

APPENDIX A: RELIABILITY OF REWEIGHTING WITH AN OVERLAP FERMION DETERMINANT

Our results presented in Sec. II, and part of the results in Sec. III, were obtained with 10^4 or 3×10^4 quenched configurations for each setting, which were reweighted with the fermion determinant of the overlap-hypercube Dirac operator. In this appendix, we discuss the reliability of this procedure by decomposing the contributions to the chiral condensate Σ (as an example), according to formula (2.5). To this end, the contributions are summed up in hierarchical order. The question is how many of the configurations, which are dominant in this respect, are needed to arrive at a good approximation of our value for Σ based on the entire statistics, i.e. how many of these configurations are statistically relevant.

In Fig. 9, we consider the percentage of dominant configurations, which is sufficient to obtain our total value of Σ up to 1%. We illustrate both the dependence on the (degenerate) fermion mass m and on the number of flavors N_{f}, i.e., the power of the fermion determinant. For low N_{f} and moderate values of m, a large fraction of the contributions is needed to obtain 99% of our Σ value; hence, the effective statistics is not much below the total data set. Vice versa, for increasing N_{f} and small m, the results are

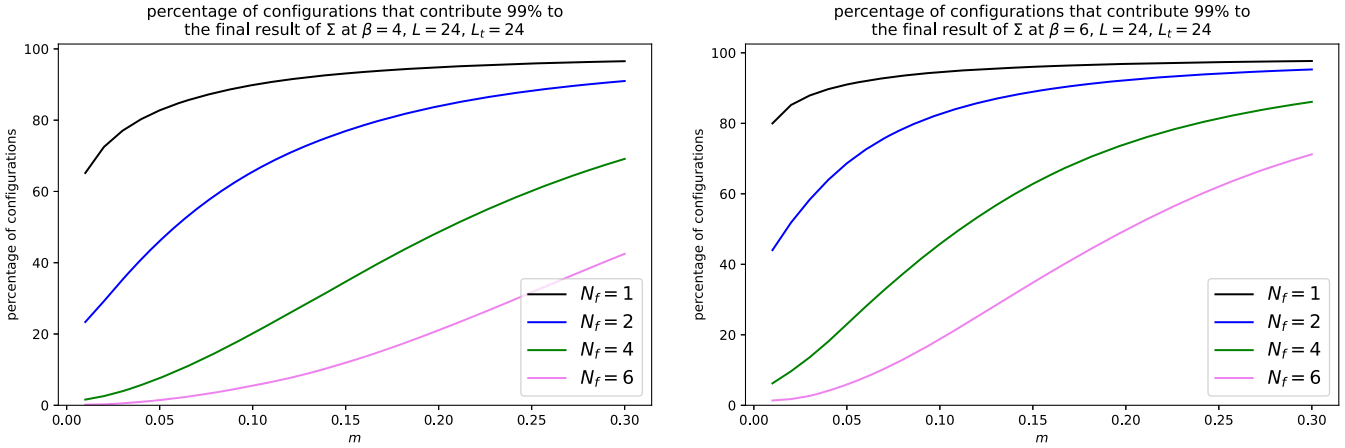

FIG. 9. The number of leading contributions which have to be included to obtain 99% of our value for the chiral condensate Σ, at $\beta = 4$ (left) and $\beta = 6$ (right), on a 24×24 lattice. For small fermion mass m and a relatively large number N_{f} of flavors, only a minor part of the configurations is necessary and therefore relevant.

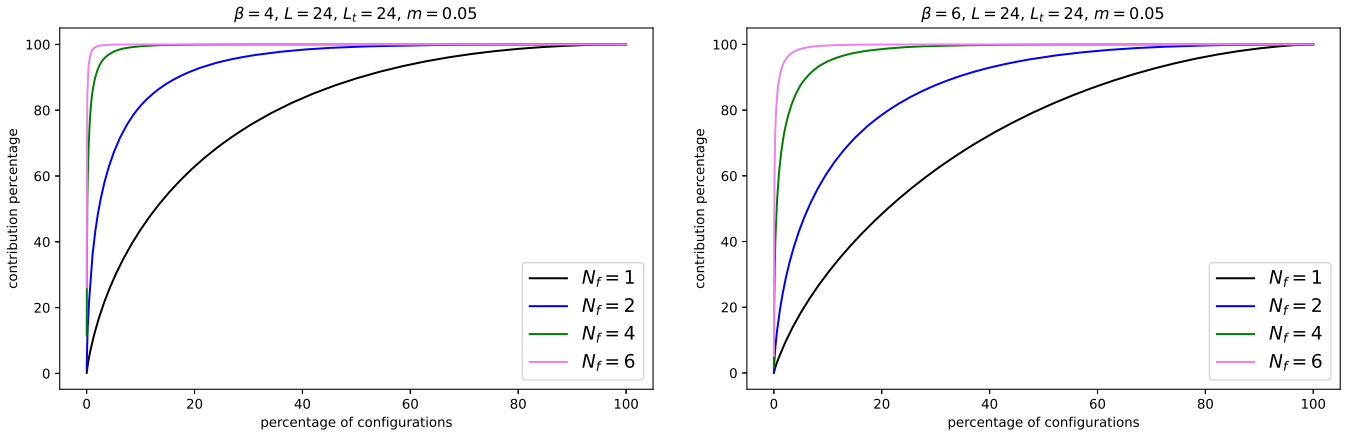

FIG. 10. The percentage of our Σ value as a function of the number of dominant contributions, out of a total of 10^4 configurations at $\beta = 4$ (left) and 3×10^4 configurations at $\beta = 6$ (right), at $m = 0.05$ on a 24×24 lattice. We see that even more flavors than 6 would be troublesome.

essentially just due to a minor subset of configurations; hence, the *effective statistics* is substantially reduced compared to the total statistics. Still, we saw in Fig. 2 that at $N_f = 2$ and $\beta = 5$ reweighting works well even down to $m = 0.001$, where the effective statistics is about 30% of the data set. On the other hand, a large number of flavors can drastically suppress the effective statistics. For instance, at $m \lesssim 0.1$, we see that $N_f > 6$ would be worrisome indeed; hence, we do not show any result for even more flavors than $N_f = 6$ in this work.

Part of our results in Secs. II and III included a minimal fermion mass of $m = 0.05$. For that particular mass, Fig. 10 shows the percentage of our Σ value as a function of the number of leading contributions. Again, we see that for a considerable N_f, in particular, for $N_f = 6$, most of our result is due to only few contributions, which confirms the limitation of the reweighting method.

APPENDIX B: THE "PION" MASS IN THE ϵ-REGIME

In Secs. II and IV, we showed simulation results obtained on $L \times L$ square lattices. In these cases, the measured "pion" mass M_π is close to its value in the thermodynamic limit ($L \to \infty$), since the condition $L \gg 1/M_\pi$ is reasonably well approximated. Down to the corresponding values for the fermion mass m, we also observed agreement of M_π calculated either with the correlation function of the density $\bar{\psi}\sigma_3\psi$, or with $\bar{\psi}\sigma_1\psi$. As usual, we refer to a Dirac operator in terms of σ_1 and σ_2, and both formulations have been used in the literature. The former is closer to the concept of the physical pion, but the latter is a valid alternative in the range of the plots in Secs. II and IV.

However, the situation changes when we proceed to even smaller values of m. Here, we enter the ϵ-regime, where it is natural that M_π is significantly enhanced by finite-size effects. Moreover, we observed that these two formulations of M_π react very differently to the squeezing in a small physical volume, as we illustrate in Fig. 11.

For the formulation with σ_3, one obtains a plateau with a residual "pion" mass $M_\pi^{\sigma_3}$, similarly to the δ-regime, which is the generic behavior. For the σ_1 formulation, however, $M_\pi^{\sigma_1}$ approaches 0, closely following the relation $M_\pi^{\sigma_1} \propto m$, which is an artifact due to the use of σ_1. In this sense, the σ_1-formulation is a valid alternative only in large volumes.

However, it is an amazing observation that $M_\pi^{\sigma_1}$ at tiny $m \lesssim 0.02$ accurately follows the prediction in Eq. (36) of Ref. [7] in the second regime, where $M_\pi L_t \ll 1$. We referred to it before in Sec. II; in that prediction, there is no residual "pion mass" because Ref. [7] deals with a large spatial size L. This is not the setting of our simulation, but

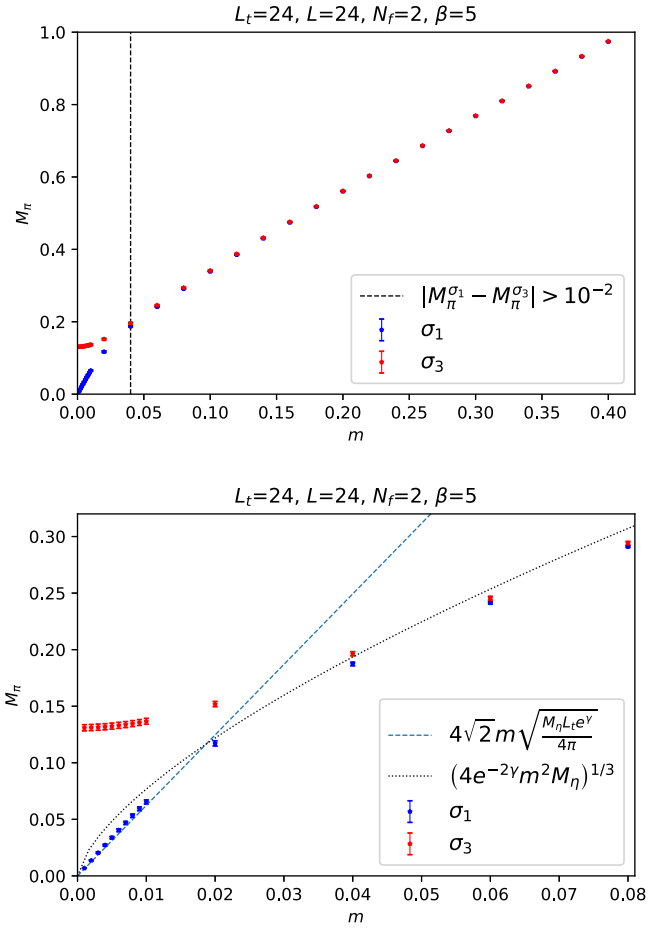

FIG. 11. Illustration of the "pion" mass measured with σ_1 ($M_\pi^{\sigma_1}$) and with σ_3 ($M_\pi^{\sigma_3}$), for $N_f = 2$, at $\beta = 5$ on a 24×24 lattice. The upper plot shows that there is good agreement at fermion mass $m \geq 0.1$, but at $m \leq 0.05$, they differ drastically: $M_\pi^{\sigma_3}$ attains a residual value, which is the expected ϵ-regime behavior, whereas $M_\pi^{\sigma_1}$ drops to 0 with an approximately linear dependence on $m \lesssim 0.02$. The lower plot zooms into the small-m region, and compares the data to Eq. (36) of Ref. [7], where $M_\eta = g\sqrt{2/\pi}$ is the "η-mass" in the chiral limit, cf. Eq. (4.4), and γ is Euler's constant. For $m \gtrsim 0.05$, $M_\pi^{\sigma_1}$ and $M_\pi^{\sigma_3}$ are close to each other, and to the prediction in the third regime of Ref. [7].

$M_\pi^{\sigma_1}$ follows this prediction to high accuracy. The reason for this observation remains to be explored.

As the fermion mass increases to $m \gtrsim 0.05$, the "pion masses" measured in both ways are close, $M_\pi^{\sigma_1} \approx M_\pi^{\sigma_3}$, and they are now in the vicinity of the third regime Eq. (36) of Ref. [7], where $M_\pi L \gg 1$, and $M_\pi \propto m^{2/3}$.

This is a technical observation, which could be of interest for future lattice studies, but it does not seem to be documented in the literature.

[1] J. Schwinger, Gauge invariance and mass. 2., Phys. Rev. **128**, 2425 (1962).

[2] S. R. Coleman, R. Jackiw, and L. Susskind, Charge shielding and quark confinement in the massive Schwinger model, Ann. Phys. (N.Y.) **93**, 267 (1975).

[3] K. Harada, T. Sugihara, M. Taniguchi, and M. Yahiro, The massive Schwinger model with $SU(2)_f$ on the light cone, Phys. Rev. D **49**, 4226 (1994).

[4] J. F. Nieto Castellanos, The 2-flavor Schwinger model at finite temperature and in the delta-regime, B.Sc. thesis, Universidad Nacional Autónoma de México, 2021.

[5] I. Hip, J. F. Nieto Castellanos, and W. Bietenholz, Finite temperature and δ-regime in the 2-flavor Schwinger model, Proc. Sci. LATTICE2021 (**2022**) 279; J. F. Nieto Castellanos, I. Hip, and W. Bietenholz, New insight in the 2-flavor Schwinger model based on lattice simulations, Rev. Mex. Fis. Suppl. **3**, 020707 (2022).

[6] A. V. Smilga, On the fermion condensate in the Schwinger model, Phys. Lett. B **278**, 371 (1992).

[7] J. Hetrick, Y. Hosotani, and S. Iso, The massive multi-flavor Schwinger model, Phys. Lett. B **350**, 92 (1995).

[8] Y. Hosotani, More about the massive multiflavor Schwinger model, in *Proceedings of the Nihon University Workshop on Fundamental Problems in Particle Physics* (1995), p. 64, arXiv:hep-th/9505168.

[9] Y. Hosotani and R. Rodriguez, Bosonized massive N-flavor Schwinger model, J. Phys. A **31**, 9925 (1998).

[10] M. Gell-Mann, R. J. Oakes, and B. Renner, Behavior of current divergences under $SU_3 \times SU_3$, Phys. Rev. **175**, 2195 (1968).

[11] H. Neuberger, Exactly massless quarks on the lattice, Phys. Lett. B **417**, 141 (1998).

[12] H. Neuberger, More about exactly massless quarks on the lattice, Phys. Lett. B **427**, 353 (1998).

[13] M. Lüscher, Exact chiral symmetry on the lattice and the Ginsparg-Wilson relation, Phys. Lett. B **428**, 342 (1998).

[14] W. Bietenholz, Solutions of the Ginsparg-Wilson relation and improved domain wall fermions, Eur. Phys. J. C **6**, 537 (1999).

[15] W. Bietenholz, Convergence rate and locality of improved overlap fermions, Nucl. Phys. **B644**, 223 (2002).

[16] W. Bietenholz and I. Hip, The scaling of exact and approximate Ginsparg-Wilson fermions, Nucl. Phys. **B570**, 423 (2000).

[17] W. Bietenholz, I. Hip, S. Shcheredin, and J. Volkholz, A numerical study of the 2-flavour Schwinger model with dynamical overlap hypercube fermions, Eur. Phys. J. C **72**, 1938 (2012).

[18] D. Landa-Marbán, W. Bietenholz, and I. Hip, Features of a 2d gauge theory with vanishing chiral condensate, Int. J. Mod. Phys. C **25**, 1450051 (2014).

[19] S. Dürr and C. Hoelbling, Staggered versus overlap fermions: A study in the Schwinger model with $N_f = 0, 1, 2$, Phys. Rev. D **69**, 034503 (2004).

[20] H. Leutwyler, Energy levels of light quarks confined to a box, Phys. Lett. B **189**, 197 (1987).

[21] P. Hasenfratz and F. Niedermayer, Finite size and temperature effects in the AF Heisenberg model, Z. Phys. B **92**, 91 (1993).

[22] P. Hasenfratz and H. Leutwyler, Goldstone boson related finite size effects in field theory and critical phenomena with $O(N)$ symmetry, Nucl. Phys. **B343**, 241 (1990).

[23] P. Hasenfratz, The QCD rotator in the chiral limit, Nucl. Phys. **B828**, 201 (2010).

[24] F. Niedermayer and P. Weisz, Matching effective chiral Lagrangians with dimensional and lattice regularization, J. High Energy Phys. 04 (2016) 110.

[25] W. Bietenholz, M. Göckeler, R. Horsley, Y. Nakamura, D. Pleiter, P. E. L. Rakow, G. Schierholz, and J. M. Zanotti, Pion in a box, Phys. Lett. B **687**, 410 (2010).

[26] M. E. Matzelle and B. C. Tiburzi, Low-energy QCD in the delta regime, Phys. Rev. D **93**, 034506 (2016).

[27] A. Smilga and J. J. M. Verbaarschot, Scalar susceptibility in QCD and the multiflavor Schwinger model, Phys. Rev. D **54**, 1087 (1996).

[28] M. Kieburg, J. J. M. Verbaarschot, and S. Zafeiropoulos, Dirac spectra of 2-dimensional QCD-like theories, Phys. Rev. D **90**, 085013 (2014).

[29] C. Gattringer and E. Seiler, Functional integral approach to the N-flavor Schwinger model, Ann. Phys. (N.Y.) **233**, 97 (1994).

[30] S. Elser, The local bosonic algorithm applied to the massive Schwinger model, Ph.D. thesis, Humboldt Universität zu Berlin, 1997, arXiv:hep-lat/0103035.

[31] L. V. Belvedere, K. D. Rothe, B. Schroer, and J. Swieca, Generalized two-dimensional Abelian gauge theories and confinement, Nucl. Phys. **B153**, 112 (1979).

[32] I. Affleck, On the realization of chiral symmetry in $(1 + 1)$ dimensions, Nucl. Phys. **B265**, 448 (1986).

[33] S. Duane, A. D. Kennedy, B. J. Pendleton, and D. Roweth, Hybrid Monte Carlo, Phys. Lett. B **195**, 216 (1987).

[34] C. Gattringer, I. Hip, and C. B. Lang, The chiral limit of the two flavor lattice Schwinger model with Wilson fermions, Phys. Lett. B **466**, 287 (1999).

[35] E. Witten, Current algebra theorems for the U(1) Goldstone boson, Nucl. Phys. **B156**, 269 (1979); G. Veneziano, U(1) without instatons, Nucl. Phys. **B159**, 213 (1979).

[36] S. Dürr, Z. Fodor, C. Hoelbling, and T. Kurth, Precision study of the SU(3) topological susceptibility in the continuum, J. High Energy Phys. 04 (2007) 055.

[37] E. Seiler and I. O. Stamatescu, Some remarks on the Witten-Veneziano formula for the η' mass, Report No. MPI-PAE/PTh 10/87, 1987.

[38] C. Bonati and P. Rossi, Topological susceptibility of two-dimensional $U(N)$ gauge theories, Phys. Rev. D **99**, 054503 (2019).

[39] W. A. Bardeen, A. Duncan, E. Eichten, and H. Thacker, Quenched approximation artifacts: A study in two-dimensional QED, Phys. Rev. D **57**, 3890 (1998).